NEURO-ONCOLOGY

Functional diffusion maps (fDMs) evaluated before and after radiochemotherapy predict progression-free and overall survival in newly diagnosed glioblastoma

Benjamin M. Ellingson, Timothy F. Cloughesy, Taryar Zaw, Albert Lai, Phioanh L. Nghiemphu, Robert Harris, Shadi Lalezari, Naveed Wagle, Kourosh M. Naeini, Jose Carrillo, Linda M. Liau, and Whitney B. Pope

Departments of Radiological Sciences (B.M.E., T.Z., R.H., K.M.N., W.B.P.), Neurology (T.F.C., A.L., P.L.N., S.L., N.W., J.C.), and Neurosurgery (L.M.L.), David Geffen School of Medicine, University of California Los Angeles, Los Angeles, California

Functional diffusion mapping (fDM) has shown promise as a sensitive imaging biomarker for predicting survival in initial studies consisting of a small number of patients, mixed tumor grades, and before routine use of anti-angiogenic therapy. The current study tested whether fDM performed before and after radiochemotherapy could predict progression-free and overall survival in 143 patients with newly diagnosed glioblastoma from 2007 through 2010, many treated with anti-angiogenic therapy after recurrence. Diffusion and conventional MRI scans were obtained before and 4 weeks after completion of radiotherapy and concurrent temozolomide treatment. FDM was created by coregistering pre- and posttreatment apparent diffusion coefficient (ADC) maps and then performing voxel-wise subtraction. FDMs were categorized according to the degree of change in ADC in pre- and posttreatment fluid-attenuated inversion recovery (FLAIR) and contrast-enhancing regions. The volume fraction of fDM-classified increasing ADC(+), decreasing ADC(−), and change in ADC(+/−) were tested to determine whether they were predictive of survival. Both Bonferroni-corrected univariate log-rank analysis and Cox proportional hazards modeling demonstrated that patients with decreasing ADC in a large volume fraction of pretreatment FLAIR or contrast-enhancing regions were statistically more likely to progress earlier and expire sooner than in patients with a lower volume fraction. The current study supports the hypothesis that fDM is a sensitive imaging biomarker for predicting survival in glioblastoma.

Keywords: biomarker, fDMs, functional diffusion maps, glioblastoma, MRI.

Corresponding Author: Benjamin M. Ellingson, PhD, Assistant Professor, Department of Radiological Sciences, David Geffen School of Medicine, University of California Los Angeles, 924 Westwood Blvd, Suite 615, Los Angeles, CA 90024 (bellingson@mednet.ucla.edu).

Malignant gliomas are the second leading cause of cancer-associated mortality among persons <35 years of age, the fourth leading cause among persons <54 years of age, and kill ~13 000 persons per year.[1] Glioblastoma is the most malignant type of glioma and has a very poor prognosis, having a mean survival of only ~14.6 months.[2] This dismal prognosis is largely attributed to tumor growth and infiltration sometimes difficult to detect by conventional MRI, making novel imaging biomarkers important for aiding in both tumor spatial localization and in predicting patient survival.

Diffusion-weighted imaging (DWI) using magnetic resonance is a valuable tool used to elicit insight into the microstructure of the underlying tissue of interest.[3] From multiple DWIs, measurements of an apparent diffusion coefficient (ADC) can be calculated, reflecting the relative magnitude of water mobility. In particular, ADC is directly proportional to the volume fraction of extracellular, freely mobile water molecules; therefore, ADC is sensitive to changes in tumor cell density,[4–6] edema, and necrosis. ADC measurements can be used in the evaluation of regions suspected of brain tumor invasion and proliferation[7] and the efficacy of specific treatment paradigms.[8] The functional diffusion map (fDM) is a method of evaluating changes in ADC known to accompany successful cytotoxic therapies.[9,10] In contrast

to other techniques that evaluate the average ADC measurements for an entire region, fDMs do not assume homogeneity in tumors. Instead, ADC maps collected on posttreatment days are coregistered with a base image at an initial pretreatment time point, and then voxel-wise changes in ADC are calculated and labeled according to the magnitude of their change. This technique has been shown to be one of the most sensitive early biomarkers for tumor response to chemotherapeutics and radiotherapy and has been shown to be highly specific to progression of high-grade gliomas;[11,12] however, this technique has only been tested in a limited number of patients and a mixture of tumor grades. In addition, these early studies were performed before routine use of anti-angiogenic therapies after tumor recurrence, calling for a re-evaluation of fDMs in the new therapeutic paradigm.

In the current study, we implemented fDMs in a large cohort ($n = 143$) of patients with glioblastoma (World Health Organization [WHO] grade IV), examining spatially specific ADC changes before and 4 weeks after completion of radiotherapy with concurrent temozolomide (radiochemotherapy) after tissue diagnosis. The usefulness of fDMs as a predictive biomarker for response to initial radiochemotherapy was tested using progression-free (PFS) and overall survival (OS) as clinical end points.

Materials and Methods

Patients

All patients participating in this study signed institutional review board–approved informed consent. Data acquisition was performed in compliance with all applicable Health Insurance Portability and Accountability Act regulations. Patients were retrospectively selected from our institution's neuro-oncology database from 1 January 2007 through 15 September 2010. Initially, a total of 169 patients who met the following criteria were selected: (1) pathology-confirmed glioblastoma, (2) treatment with standard external beam radiotherapy (typically in 2 Gy fractions given once daily for 5 days over a 6-week period, totaling 60 Gy) and concomitant temozolomide (75 mg/m^2/day, 7 days per week during radiotherapy, followed by a 4-week break, then 6–12 cycles of adjuvant therapy at 150 mg/m^2/day to 200 mg/m^2/day), and (3) baseline (postsurgical, preradiochemotherapy) and minimum of 1 follow-up MRI scan after radiochemotherapy. The mean age ($\pm$ standard deviation) of this population was 58.4 $\pm$ 11 years, mean Karnofsky performance status (KPS; $\pm$ standard error of the mean [SEM]) was 86 (± 10), and 97 (57%) of the 169 patients were male. Seventy patients had a gross total resection (GTR) at the time of initial surgery, 73 patients had a subtotal resection (STR), and 26 patients had only a biopsy prior to radiochemotherapy. Of the initial 169 patients enrolled, 104 (62%) were given bevacizumab after recurrence, ranging from 26 to 300 days after initial

radiotherapy. Of all patients enrolled, 143 patients had good quality diffusion-weighted images before and after initiation of radiochemotherapy. Exclusions were based on gross geometric distortions or low signal-to-noise ratio in the raw DWI datasets. Baseline scans were obtained ~1 week before treatment (mean $\pm$ SEM, 8 $\pm$ 1.4 days). Follow-up scans were obtained ~10 weeks from the time of treatment initiation (mean $\pm$ SEM, 75 $\pm$ 2.6 days) or ~4 weeks from the end of initial radiochemotherapy. At the time of last assessment (July 2011), 118 of the 143 patients had died.

MRI

Data were collected on 1.5T MR systems (General Electric Medical Systems; Siemens Medical Solutions) using pulse sequences supplied by the scanner manufacturer. Standard anatomical MRI sequences included axial T1-weighted (TE/TR = 15 ms/400 ms, slice thickness = 5 mm with 1 mm interslice distance, number of excitations [NEX] = 2, matrix size = 256 × 256, and field-of-view [FOV] = 24 cm), T2-weighted fast spin-echo (TE/TR = 126–130 ms/4000 ms, slice thickness = 5 mm with 1 mm interslice distance, NEX = 2, matrix size = 256 × 256, and FOV = 24 cm), and fluid-attenuated inversion recovery (FLAIR) images (TI = 2200 ms, TE/TR = 120 ms/4000 ms, slice thickness = 5 mm with 1 mm interslice distance, NEX = 2, matrix size = 256 × 256, and FOV = 24 cm). DWIs were collected with TE/TR = 102.2 ms/8000 ms, NEX = 1, slice thickness = 5 mm with 1 mm interslice distance, matrix size = 128 × 128 (reconstructed images were zero-padded and interpolated to 256 × 256) and a FOV = 24 cm using a twice-refocused spin echo echo planar preparation.[12,13] ADC images were calculated from acquired DWIs with $b = 1000$ s/mm^2 and $b = 0$ s/mm^2 images. In addition, gadopentetate dimeglumine–enhanced (Magnevist; Berlex; 0.1 mmol/kg) axial and coronal T1-weighted images (T1 + C; coronal: TE/TR = 15 ms/400 ms, slice thickness 3 mm with 1 mm interslice distance, NEX = 2, a matrix size of 256 × 256, and FOV = 24 cm) were acquired after contrast injection.

Image Registration

All images for each patient were registered to their own pretreatment, precontrast, T1-weighted image with use of a mutual information algorithm and a 12-degree of freedom transformation with use of FSL (FMRIB; http://www.fmrib.ox.ac.uk/fsl/). Fine registration (1–2 degrees and 1–2 voxels) was then performed using a Fourier transform-based, 6-degree of freedom, rigid body registration algorithm,[14] incorporated as part of the freely available Analysis of Functional NeuroImages software package (AFNI; http://afni.nimh.nih.gov/afni). This was followed by visual inspection to ensure adequate alignment. All images were interpolated to the resolution of baseline T1-weighted images using trilinear interpolation. In cases in which

significant mass effect was an issue, attempts were made to align tumor regions exclusively. Regions of obvious misregistration (eg, near ventricles or edge of the brain) were excluded from final fDM analysis.

fDM Calculation

After proper registration was visually verified, voxel-wise subtraction was performed between ADC maps acquired posttreatment and baseline, pretreatment ADC maps. Individual voxels were stratified into 3 categories based on the change in ADC relative to the baseline ADC map. Red voxels represented areas where ADC increased beyond a ΔADC threshold of 0.4 mm^2/ms, or ADC(+), and blue voxels represented areas where ADC decreased beyond a ΔADC threshold of 0.4 mm^2/ms, or ADC(−). These ΔADC thresholds ($\pm$ 0.40 mm^2/ms) represent the 95% confidence interval for a mixture of normal-appearing gray and white matter in 69 patients with various tumor grades and follow-up time intervals ranging from 1 week to 1 year postbaseline.[6] These thresholds have been calibrated with respect to change in cell density in treatment-naive gliomas ($\pm$ 3960 nuclei/mm^2) in a previous publication.[6] In addition, the volume fraction of total changing voxels, defined as ADC(+/−) = ADC(+) + ADC(−), was quantified.

Region of Interest (ROI) Determination

In the current study, we chose to apply fDMs to regions of FLAIR signal abnormality and contrast-enhancement (T1 + C) on both pre- and posttreatment images. FLAIR ROIs have previously been used in interpreting fDM results in nonenhancing and enhancing tumors,[6,15–18] because tumor infiltration into normal brain parenchyma typically results in an increase in T2-weighted or FLAIR abnormal signal.[19–22] Furthermore, multiple investigations have suggested that T2 signal abnormalities should be routinely used to visualize the extent of malignant infiltrating tumor.[23–27] In addition, regions of contrast-enhancement (T1 + C) have also been used in fDM analyses.[9–12] FDM analysis was performed in all 143 patients, along with a subgroup fDM analysis in patients who had significant residual tumor burden. Specifically, patients with STR (defined as having a significant volume of residual contrast-enhancing tumor burden) or a diagnostic biopsy were examined separately. The mean volume of contrast-enhancement, which included postsurgical changes along the resection cavity, for GTR was 4.4 cc (median, 1.1 cc) and STR was 12.2 cc (median, 10.7 cc). Patients who had a diagnostic biopsy prior to radiochemotherapy, instead of GTR or STR, had a mean volume of contrast-enhancement of 23.6 cc. The distribution of contrast-enhancing volumes was statistically different among these 3 groups (1-way analysis of variance, $P < .0001$), and the enhancing volume defined in GTR was significantly smaller than that for patients with STR (Tukey's test, $P < .05$).

Definition of Disease Progression

Progression was defined prospectively by the treating neuro-oncologists (T.F.C., A.L., and P.L.N.). To decrease the likelihood of declaring progression in the context of pseudoprogression, the postradiation scan was considered to be the baseline scan for evaluating tumor progression. If subsequent scans showed a definite increase in imaging evaluable tumor ($\geq$25% increase in the sum of enhancing lesions, new enhancing lesion >1 cm^2, an unequivocal qualitative increase in noncontrast-enhancing tumor, or unequivocal new area of noncontrast-enhancing tumor), progression was declared at that time. Progression was determined using the first postradiation therapy scan only if a new lesion >1 cm^2 was identified outside the radiation field. Change in steroid dosage was taken into consideration before defining progression. Patients who did not meet these imaging criteria for progression but had significant neurologic decline were declared to be progressed at the time of irreversible decline. Patients who died before evidence of imaging progression were defined as progressed on the date of death.

Hypothesis Testing

To determine whether fDMs calculated before and after radiochemotherapy are valuable biomarkers for stratifying PFS and OS in patients with newly diagnosed glioblastoma, we performed a series of univariate log-rank statistical analyses on Kaplan-Meier data. Specifically, we tested whether stratifying patients by median fractional fDM change, using a single ΔADC threshold of 0.40 mm^2/ms, was a significant predictor of PFS and OS from the time of diagnosis. We hypothesized that the median volume fraction of tissue showing a decrease in ADC, or relatively hypercellular tissue, would result in a significantly shorter PFS and OS in patients with glioblastoma. On the basis of previous fDM studies, we also hypothesized that the median volume fraction of tissue showing an increase in ADC, or relatively hypocellular tissue, would result in a significantly longer PFS and OS in patients with glioblastoma. FDM analysis was performed independently by 2 investigators (T.Z. and R.H.) blinded from the survival data.

Multiple Comparisons Correction.—Bonferroni correction to the level of significance ($\alpha = 0.05$) was performed to account for the multiple testing between potential imaging biomarkers. Examining a total of 3 fDM metrics (ADC[+], ADC[−], and ADC^{+/−}) in 4 ROIs (pretreatment FLAIR, posttreatment FLAIR, pretreatment T1 + C, and posttreatment T1 + C) and 2 end points (PFS and OS) results in a total of 24 comparisons and a Bonferroni-corrected level of significance ($\alpha_{Bonferroni} = 0.002$).

Cox Proportional Hazards Model.—Cox proportional hazards models were constructed to describe PFS and OS on the basis of clinical metrics (age and KPS) combined with the top-performing fDM biomarkers, as

determined by statistical significance in Bonferonni-corrected, univariate log-rank analysis. $P = .05$ was considered to be statistically significant.

Results

Qualitatively, fDMs created by using the pretreatment and posttreatment ADC maps appeared to suggest that patients with a high volume of tissue with decreasing ADC (ie, ADC[−]) had a shorter PFS and OS, compared with patients with a lower volume of tissue with decreasing ADC. This is consistent with the hypothesis that a high volume of decreasing ADC may reflect an increase in tumor cell density indicative of ineffective treatment. Alternatively, patients with a high volume of tissue with increasing ADC (ie, ADC[+]) appeared to be more likely to progress later and live longer than patients with a lower volume of tissue with increasing ADC. This is consistent with the hypothesis that a high volume of tissue with increasing ADC largely reflects the destruction of highly cellular tumor regions, suggesting successful cytotoxic treatment. Figure 1 shows representative

fDMs using each of the 4 ROIs in 3 patients with increasing PFS and OS, showing these qualitative observations.

PFS

Consistent with qualitative observations, univariate log-rank analysis of Kaplan-Meier curves determined that patients with a decrease in ADC in a large fraction of pretreatment FLAIR regions ($\%ADC[-]^{Pre-Tx}_{FLAIR} > 20\%$) were significantly more likely to have a shorter PFS than patients with $\%ADC(-)^{Pre-Tx}_{FLAIR} < 20\%$, after Bonferroni correction (log-rank, $P = .0004$) (Fig. 2A). This was also observed in patients with a significant volume of residual enhancement after surgical intervention (patients with STR or biopsy only; 58 patients with pretreatment FLAIR abnormality; log-rank, $P = .0033$). Tumors presenting with an increase in ADC in >20% of posttreatment FLAIR regions ($\%ADC[+]^{Post-Tx}_{FLAIR} > 20\%$) had a significant PFS advantage, compared with tumors with $\%ADC(+)^{Post-Tx}_{FLAIR} < 20\%$ (log-rank, $P = .0014$) (Fig. 2E). After accounting for multiple comparisons
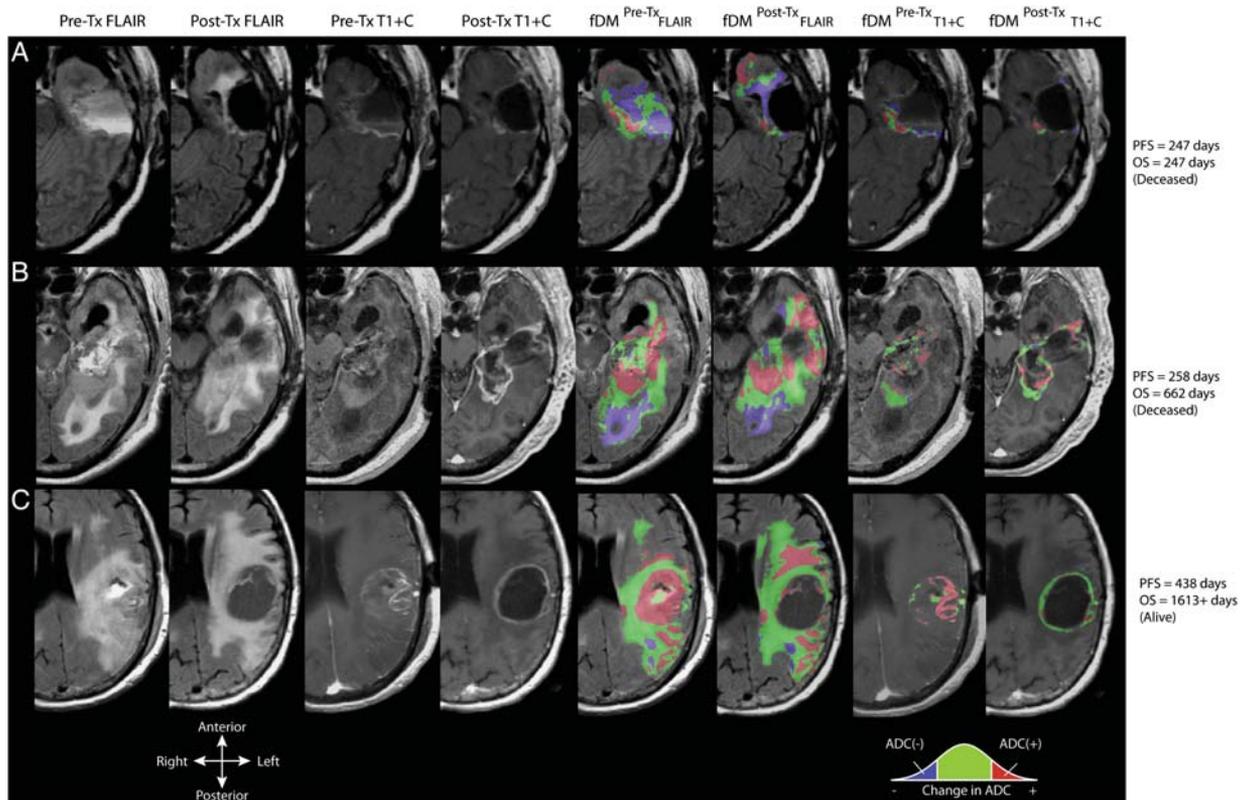

Fig. 1. Anatomical MRIs and functional diffusion maps (fDMs) for 3 patients with glioblastoma. From left column to right column: pretreatment fluid-attenuated inversion recovery (FLAIR); posttreatment FLAIR; pretreatment, postcontrast T1-weighted images (T1 + C); posttreatment T1 + C; fDMs in pretreatment FLAIR regions of interest (ROIs); fDMs in posttreatment FLAIR ROIs; fDMs in pretreatment T1 + C ROIs; and posttreatment T1 + C ROIs. (A) Patient with a short progression-free survival (PFS) and overall survival (OS), demonstrating a large volume fraction of voxels with decreased ADC (*blue*) relative to pretreatment ADC maps. (B) Patient with a short PFS but relatively longer OS demonstrates a mixed response of both voxels with a significant increase in ADC (*red*) and decrease in ADC (*blue*). (C) Long-term survival patient demonstrating a large volume fraction of tissue with increased ADC (*red*) and a small volume fraction of tissue with decreased ADC (*blue*).
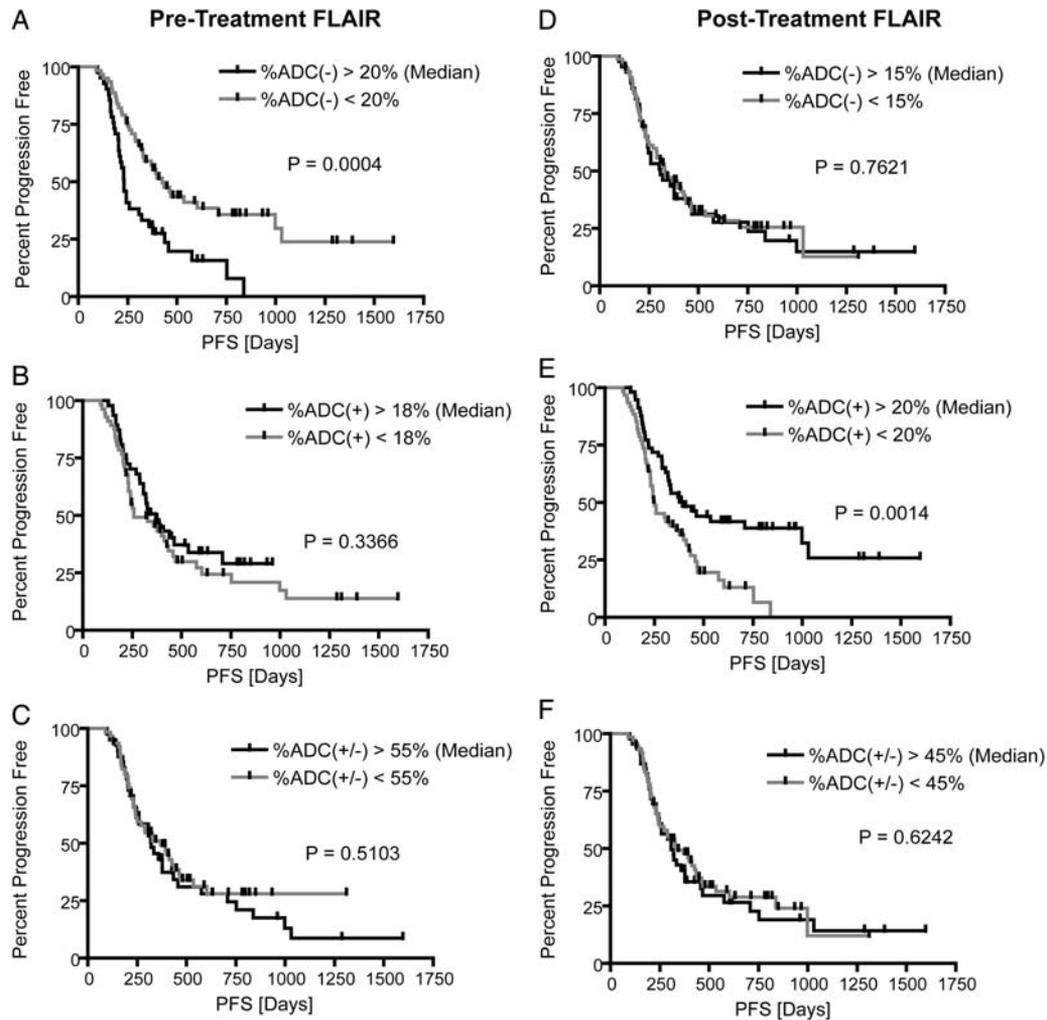
Fig. 2. Kaplan–Meier curves for progression-free survival (PFS) using functional diffusion map (fDM) metrics in FLAIR regions of interest (ROIs). (A) Relative volume fraction of tissue within pretreatment FLAIR ROIs exhibiting a significant decrease in ADC [ADC(−)]. (B) Relative volume fraction of tissue within pretreatment FLAIR ROIs exhibiting a significant increase in ADC [ADC(+)]. (C) Relative volume fraction of tissue within pretreatment FLAIR ROIs exhibiting any significant change in ADC [ADC(+/−)]. (D) Relative volume fraction of tissue within posttreatment FLAIR ROIs exhibiting a significant decrease in ADC [ADC(−)]. (E) Relative volume fraction of tissue within posttreatment FLAIR ROIs exhibiting a significant increase in ADC [ADC(+)]. (F) Relative volume fraction of tissue within posttreatment FLAIR ROIs exhibiting any significant change in ADC [ADC(+/−)].

using Bonferroni correction, a trend was also observed in patients with significant residual enhancing tumor after surgical intervention (patients with STR or biopsy only; 68 patients with posttreatment FLAIR abnormality; $P = .0303$). In addition, tumors exhibiting a decrease in ADC in >15% of pretreatment or posttreatment contrast-enhancing regions ($\%ADC[-]^{Pre-Tx}_{T1+C}$ and $\%ADC[-]^{Post-Tx}_{T1+C}$) had a shorter PFS, although comparisons were not significant after Bonferroni correction (log-rank, $P = .0031$ and $P = .0033$, respectively) (Fig. 3). Univariate results for PFS are further summarized in Table 1.

A Cox proportional hazards model consisting of age, KPS, $\%ADC(-)^{Pre-Tx}_{FLAIR} > 20\%$, $\%ADC(+)^{Post-Tx}_{FLAIR} < 20\%$, $\%ADC(-)^{Pre-Tx}_{T1+C} > 15\%$, and $\%ADC(-)^{Post-Tx}_{T1+C} > 15\%$ significantly predicted PFS (Cox model fit, $\chi^2 = 24.4$, $P = .0004$).

Results suggest that patients with a decrease in ADC in pretreatment FLAIR regions ($\%ADC[-]^{Pre-Tx}_{FLAIR} > 15\%$) had a significantly shorter PFS (Cox regression, hazard ratio $= 2.63$, $P = .0003$), whereas other factors, including age and KPS, were not found to be significant predictors of PFS (Table 2).

OS

Patients with a decrease in ADC <15% ($\%ADC[-]^{Pre-Tx}_{T1+C} < 15\%$; log-rank, $P = .0002$) or a volume fraction of tissue with changing ADC >50% ($\%ADC[+/-]^{Pre-Tx}_{T1+C} > 50\%$; log-rank, $P = .0002$) in pretreatment contrast-enhancing regions had a longer OS, compared with either $\%ADC(-)^{Pre-Tx}_{T1+C} > 15\%$ or $\%ADC(+/-)^{Pre-Tx}_{T1+C} < 50\%$, respectively. A Cox
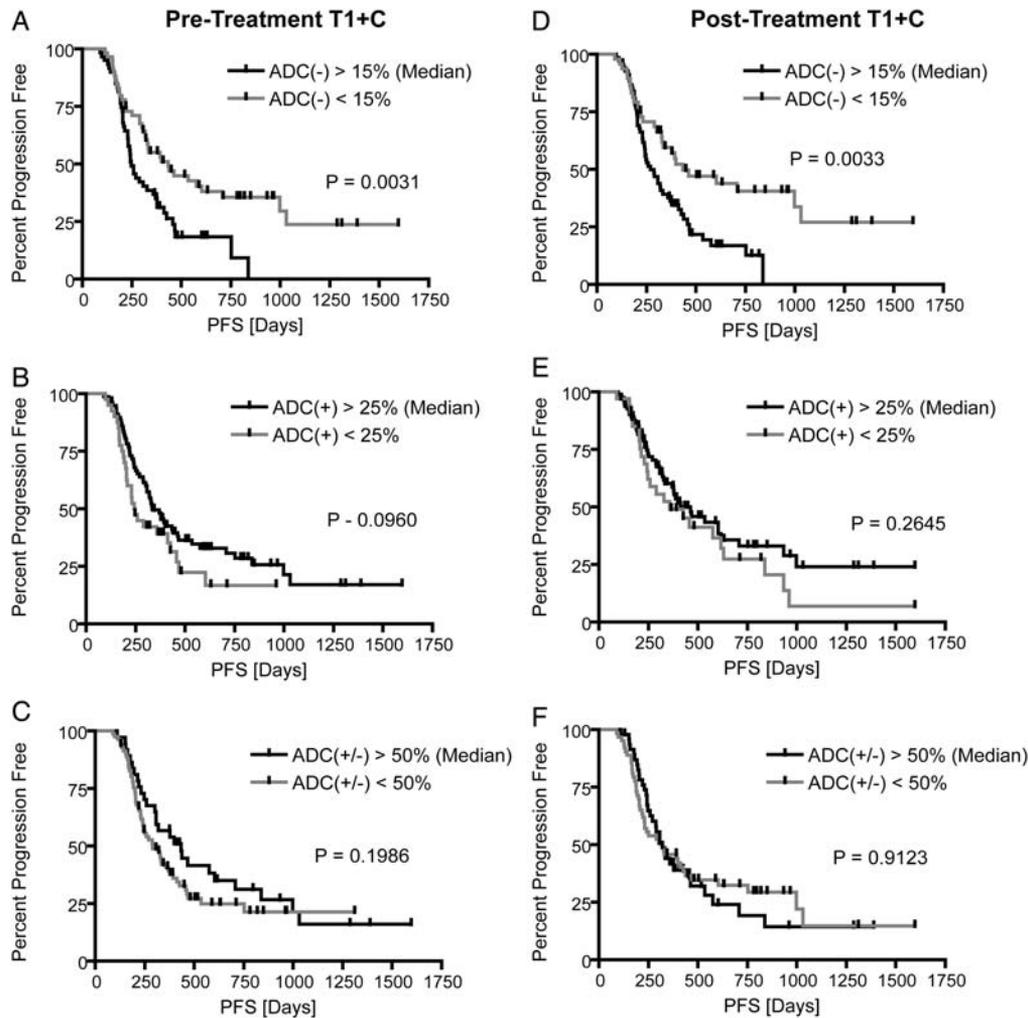
Fig. 3. Kaplan-Meier curves for progression-free survival (PFS) using functional diffusion map (fDM) metrics within T1 + C regions of interest (ROIs). (A) Relative volume fraction of tissue within pretreatment T1 + C ROIs exhibiting a significant decrease in ADC [ADC(−)]. (B) Relative volume fraction of tissue within pretreatment T1 + C ROIs exhibiting a significant increase in ADC [ADC(+)]. (C) Relative volume fraction of tissue within pretreatment T1 + C ROIs exhibiting any significant change in ADC [ADC(+/−)]. (D) Relative volume fraction of tissue within posttreatment T1 + C ROIs exhibiting a significant decrease in ADC [ADC(−)]. (E) Relative volume fraction of tissue within posttreatment T1 + C ROIs exhibiting a significant increase in ADC [ADC(+)]. (F) Relative volume fraction of tissue within posttreatment T1 + C ROIs exhibiting any significant change in ADC [ADC(+/−)].

proportional hazards model confirmed that $\%ADC(-)^{Pre-Tx}_{T1+C} > 15\%$ was a statistically significant predictor of OS (Cox regression, hazard ratio = 3.15; $P < .0001$) (Table 2).

When examining patients with a significant enhancing tumor burden after surgical intervention (STR or biopsy), patients with a decreasing ADC in a large volume fraction of pretreatment or posttreatment contrast-enhancing regions had a significantly shorter OS, compared with patients exhibiting a low volume fraction ($\%ADC[-]^{Pre-Tx}_{T1+C} > 15\%$; STR or biopsy only; $n = 68$; log-rank, $P < .0001$; $\%ADC[-]^{Post-Tx}_{T1+C} > 15\%$; log-rank, $P = .0016$). This was also observed in pretreatment FLAIR regions ($\%ADC[-]^{Pre-Tx}_{FLAIR} > 20\%$; STR or biopsy only; $n = 58$; log-rank, $P = .0005$). Patients with significant enhancing tumor burden after surgical

intervention who also had a large percentage of the pretreatment or posttreatment enhancing mass with a changing ADC trended toward a longer OS ($\%ADC[+/-]^{Pre-Tx}_{T1+C} > 50\%$; STR or biopsy only; $n = 69$; log-rank, $P = .0095$; $\%ADC[+/-]^{Post-Tx}_{T1+C} > 50\%$; log-rank, $P = .0034$).

Discussion

Voxel-based analyses of physiological imaging parameters are highly sensitive methods for localizing and quantifying treatment response when tumors are spatially heterogeneous. Preliminary fDM studies have shown promise as an early predictive biomarker for a variety of tumor grades and using single ROIs.[10,12,28] The

Table 1. FDM performance in pre- and posttreatment fluid-attenuated inversion recovery (FLAIR) and contrast-enhancing (T1 + C) regions of interest (ROIs)

	Pretreatment FLAIR ROI (n = 143)			Posttreatment FLAIR ROI (n = 141)		
	ADC(−)	ADC(+)	ADC(+/−)	ADC(−)	ADC(+)	ADC(+/−)
Median Volume Fraction [%]	20%	18%	55%	15%	20%	45%
Median PFS Difference [Days]	194	110	48	24	142	24
Log-Rank P-Value	P = .0004*	P = .3366	P = .5103	P = .7621	P = .0014*	P = .6242
Hazard Ratio(+/−95%C.I.)	2.2 (1.5–4.3)	1.3 (0.8–2.0)	1.2 (0.7–1.8)	1.1 (0.7–1.7)	2.0 (1.3–3.2)	1.1 (0.7–1.7)
Median OS Difference [Days]	336	42	10	39	33	103
Log-Rank P-Value	P = .0026	P = .9658	P = .7926	P = .9729	P = .8471	P = .5092
Hazard Ratio (+/−95%C.I.)	2.1 (1.4–4.2)	1.0 (0.6–1.7)	1.0 (0.6–1.6)	1.0 (0.6–1.6)	1.0 (0.3–1.6)	1.2 (0.7–1.9)
	Pre-Treatment T1 + C ROI (n = 141)			Post-Treatment T1 + C ROI (n = 139)		
	ADC(−)	ADC(+)	ADC(+/−)	ADC(−)	ADC(+)	ADC(+/−)
Median Volume Fraction [%]	15%	25%	50%	15%	25%	50%
Median PFS Difference [Days]	187	91	144	163	105	2
Log-Rank P Value	P = .0031*	P = .0960	P = .1986	P = .0033*	P = .2645	P = .9123
Hazard Ratio (+/−95%C.I.)	1.8 (1.3–3.1)	1.5 (0.9–2.5)	1.3 (0.9–2.1)	1.9 (1.3–3.1)	1.3 (0.8–2.3)	1.0 (0.7–1.6)
Median OS Difference [Days]	410	203	518	378	90	222
Log-Rank P Value	P = .0002*	P = .0066	P = .0002*	P = .0028	P = .2218	P = .0661
Hazard Ratio (+/−95% CI)	2.3 (1.6–4.3)	1.9 (1.2–3.8)	2.5 (1.6–4.2)	2.0 (1.3–3.5)	1.1 (0.5–1.8)	1.6 (1.0–2.7)

*Statistically significant P values in log-rank univariate analysis after Bonferroni correction.

Table 2. Cox proportional hazards model results

Variable	PFS Cox Regression Analysis (n = 139)		
	Cox Model Risk Ratio	χ^2 = 24.4 Coefficient	P = .0004 P-value
Age [Years]	1.0023	0.0023	.7948
KPS	0.9949	−0.0051	.5786
ADC(−)$^{Pre-Tx}_{FLAIR}$ > 20%	2.6282	0.9663	.0003***
ADC(+)$^{Post-Tx}_{FLAIR}$ > 20%	1.2758	0.2436	.3018
ADC(−)$^{Pre-Tx}_{T1+C}$ > 15%	0.9777	−0.0226	.9401
ADC(−)$^{Pre-Tx}_{T1+C}$ > 15%	0.8385	−0.1761	.5356
	OS Cox Regression Analysis (n = 139)		
	Cox Model Risk Ratio	χ^2 = 26.6 Coefficient	P < .0001 P value
Age [Years]	0.9969	−0.0032	.7589
KPS	1.0037	0.0036	.7374
ADC(−)$^{Pre-Tx}_{T1+C}$ > 15%	3.1521	1.1481	<.0001***
ADC(−)$^{Pre-Tx}_{T1+C}$ < 50%	1.0082	0.0082	.9684

*P < .05; **P < .01; ***P < .001.

current study represents the largest, most comprehensive fDM study to date, examining a total of 143 patients with de novo glioblastoma treated with radiochemotherapy using a total of 4 different ROIs.

The current study suggests that patients with a decrease in ADC 4 weeks after completion of radiochemotherapy >20% of FLAIR or >15% of contrast-enhancing regions are more likely to progress sooner and live shorter, respectively, compared with patients with a lower volume fraction of tumor with decreasing ADC. This effect may be attributable to a number of biological factors, including increased gliosis and/or reactive cells, a decrease in the volume extent of edematous tissue, a decrease in vascular permeability, an increase in intracellular volume because of cell swelling, or an increase in cell density because of proliferating tumor cells. For example, an increase in reactive astrocytic projections (gliosis) and/or an increase in macrophages as a result of injury to the brain during radiochemotherapy is thought to cause a decrease in ADC because of an increase in extracellular tortuosity and an increase in physical boundaries to water diffusion; however, these biological changes are more likely to contribute to an increase in PFS and/or OS as opposed to the decrease in PFS and/or OS observed in the current study. Similarly, a decrease in the volume extent of edematous tissue or a decrease in vascular permeability could have caused a decrease in ADC, because the extracellular space is thought to have more mobile water molecules and contribute more to the estimate of ADC using the current DWI parameters, but a large decrease in edema or vascular permeability after treatment is traditionally thought to be favorable and not result in a shorter PFS or OS. Thus, it is most likely that a large extent of FLAIR or T1 + C showing a decrease in ADC after radiochemotherapy may reflect an increase in tumor cellularity as a result of ineffective therapy; however, pathological confirmation is needed to confirm this hypothesis.

Previous fDM in radiochemotherapy studies had substantial limitations,[10,12,28] including an examination of a relatively heterogeneous patient population (all malignant gliomas), relatively small sample size (40–66 patients), a single region of interest/mask (contrast-enhancing regions exclusively), and a relatively arbitrary ADC threshold for fDM classification (0.55 μm²/ms,
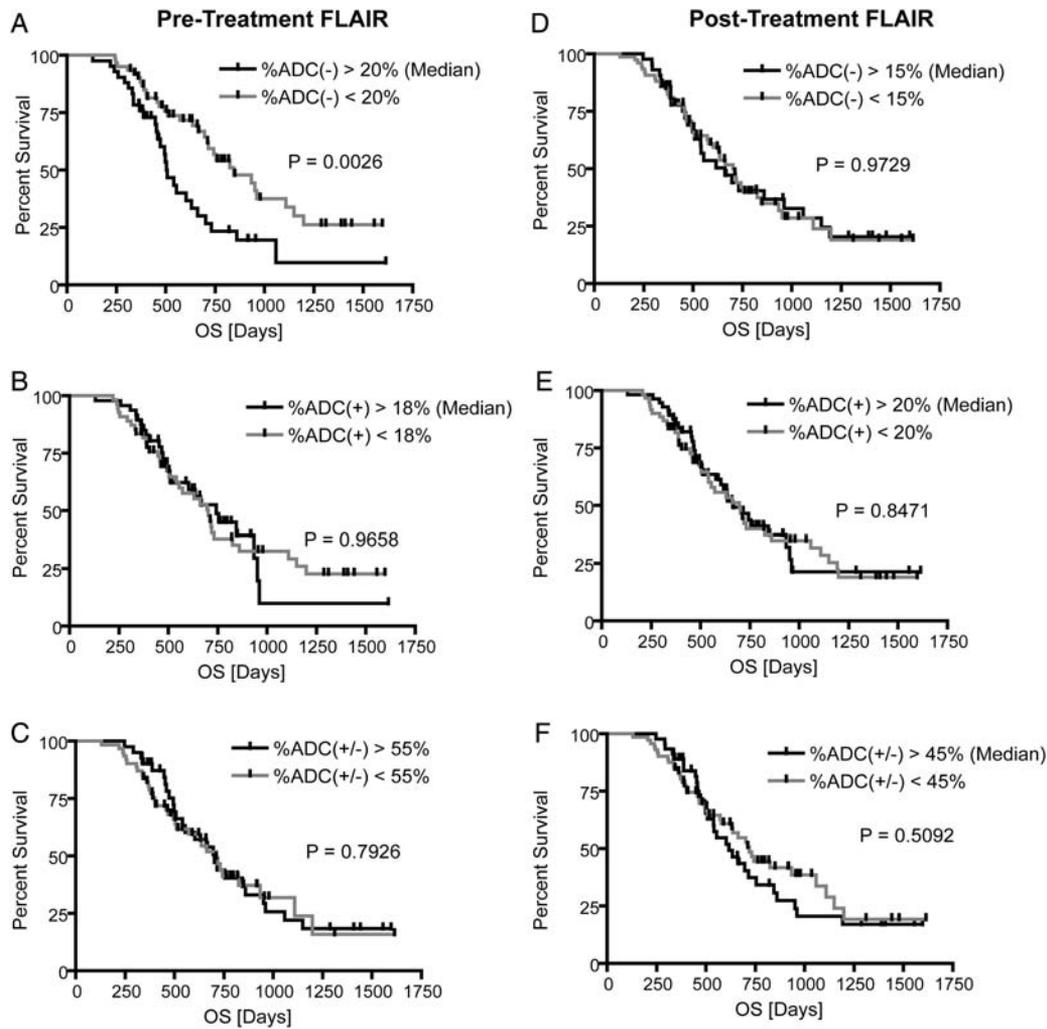
Fig. 4. Kaplan-Meier curves for overall survival (OS) using functional diffusion map (fDM) metrics within FLAIR regions of interest (ROIs). (A) Relative volume fraction of tissue within pretreatment FLAIR ROIs exhibiting a significant decrease in ADC [ADC(−)]. (B) Relative volume fraction of tissue within pretreatment FLAIR ROIs exhibiting a significant increase in ADC [ADC(+)]. (C) Relative volume fraction of tissue within pretreatment FLAIR ROIs exhibiting any significant change in ADC [ADC(+/−)]. (D) Relative volume fraction of tissue within posttreatment FLAIR ROIs exhibiting a significant decrease in ADC [ADC(−)]. (E) Relative volume fraction of tissue within posttreatment FLAIR ROIs exhibiting a significant increase in ADC [ADC(+)]. (F) Relative volume fraction of tissue within posttreatment FLAIR ROIs exhibiting any significant change in ADC [ADC(+/−)].

based on empirical data in 15 patients). In addition, previous fDM studies used ADC maps collected before and during radiotherapy (3 weeks after initiation of treatment), which does not represent the standard of care for clinical monitoring of malignant gliomas. Similarly, previous fDM studies were performed before routine use of anti-angiogenic therapies in recurrent glioblastoma, which is now the standard of care for patients in the United States.

Any one these factors may have contributed to observed differences between the current study and previous fDM studies in radiochemotherapy.

The current study supports the hypothesis that fDMs are a predictive imaging biomarker of patient survival in glioblastoma. In particular, patients who exhibited a decrease in ADC >0.4 $\mu m^2/ms$ in $>20\%$ of pretreatment

FLAIR abnormal regions or $>15\%$ of pretreatment contrast-enhancing regions had significantly shorter PFS and OS, respectively.

Technical Limitations and Considerations

The use of standard, clinical diffusion magnetic resonance sequence parameters poses some potential limitations. Specifically, according to the recommendations of the National Cancer Institute Diffusion MRI Consensus Conference,[29] ≥ 3 b values (0 s/mm², >100 s/mm², and >500 s/mm²) should be used for estimation of perfusion-insensitive ADC. Because of the retrospective nature of the current study, we have used only $b = 0$ and $b = 1000$ s/mm² images. Previous
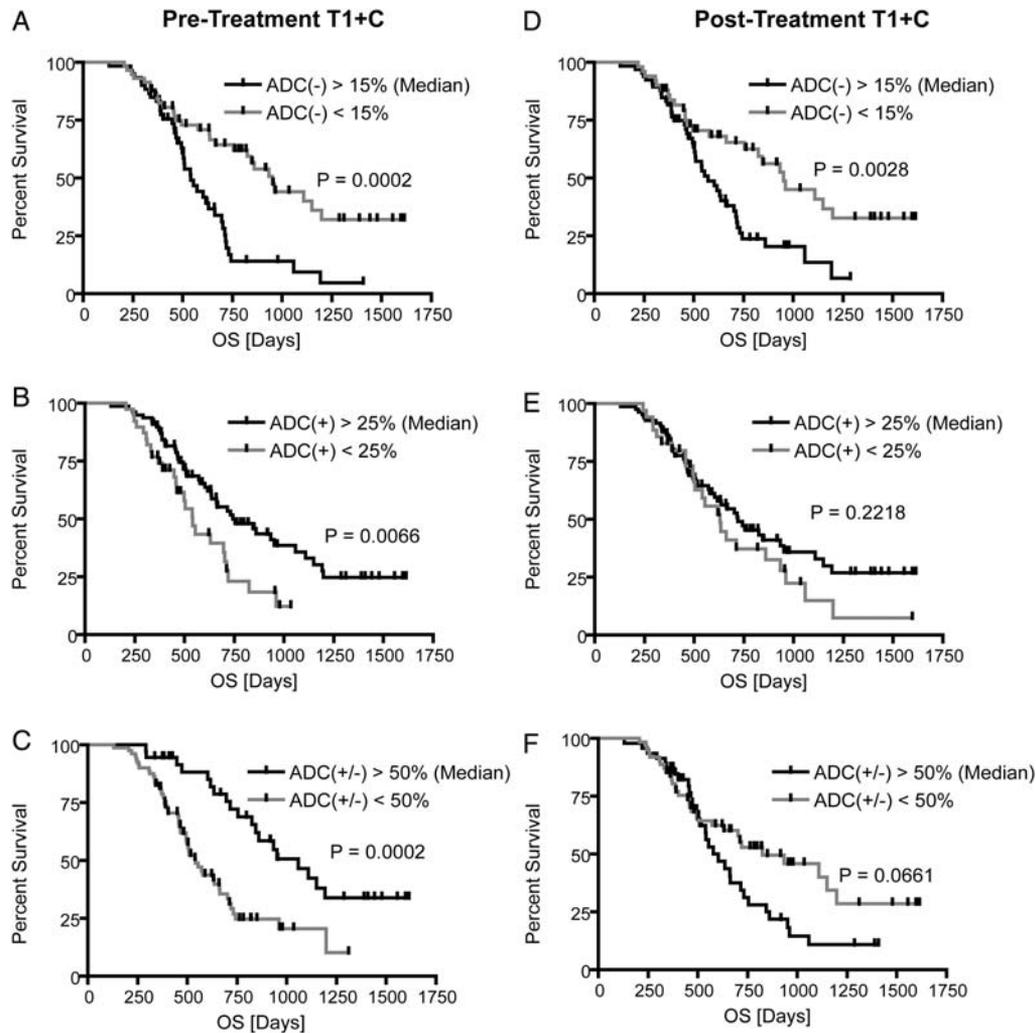
Fig. 5. Kaplan–Meier curves for overall survival (OS) using functional diffusion map (fDM) metrics within T1 + C regions of interest (ROIs). (A) Relative volume fraction of tissue within pretreatment T1 + C ROIs exhibiting a significant decrease in ADC [ADC(−)]. (B) Relative volume fraction of tissue within pretreatment T1 + C ROIs exhibiting a significant increase in ADC [ADC(+)]. (C) Relative volume fraction of tissue within pretreatment T1 + C ROIs exhibiting any significant change in ADC [ADC(+/−)]. (D) Relative volume fraction of tissue within posttreatment T1 + C ROIs exhibiting a significant decrease in ADC [ADC(−)]. (E) Relative volume fraction of tissue within posttreatment T1 + C ROIs exhibiting a significant increase in ADC [ADC(+)]. (F) Relative volume fraction of tissue within posttreatment T1 + C ROIs exhibiting any significant change in ADC [ADC(+/−)].

studies involving fDMs have used similar levels of diffusion weighting without significant issues with interpretation. In addition, the use of clinical diffusion magnetic resonance sequences for fDM analysis may be confounded by other pathologies, including ischemic events, or other treatments, including steroid use. Thus, clinical use of fDMs should involve interpretation from clinicians to rule out the possibility of these confounding factors.

The use of a rigid-body image registration algorithm to align serial ADC maps to baseline ADC maps poses another potential limitation. Significant mass effect from tumor growth or intracranial pressure induced by edema may cause inaccuracies in the registration between diffusion MRI datasets. Ellingson et al.[30] recently demonstrated an increase

in clinical sensitivity by incorporating nonlinear registration into the fDM processing pipeline. Although the current study did not use nonlinear (elastic) registration, we chose to overcome many of the challenges by using 2 sequential automated registration steps, followed by manual inspection. In addition, regions suspected of containing cerebrospinal fluid contamination from image misregistration near boundaries of tissue mismatch were excluded. Of note, no studies have evaluated the spatial accuracy of fDM-classified image voxels. Therefore, whether the precise voxels represented in the fDMs have actually physically changed or whether they are the same tissues in the voxel before and after therapy is an important question that is not directly addressed in the current study.

Another limitation in the current study was the use of progression as a clinical end point for evaluation. Progression, in general, is considered to be a relatively soft clinical end point. However, in the current study, we chose to use a prospective determination of progression, because it was an unbiased estimate of disease recurrence.

Conclusion

In summary, the current study represents the largest, most comprehensive fDM study in de novo glioblastoma to date ($n = 143$). Results support the hypothesis that fDM is a sensitive imaging biomarker for predicting survival in glioblastoma, suggesting patients exhibiting a large volume of tissue with decreased

ADC are statistically more likely to have a short PFS and OS.

References

1. CBTRUS. Primary Brain Tumors in the United States 2000–2004. Chicago, IL: Central Brain Tumor Registry of the United States; 2008.

2. Stupp R, Mason WP, van den Bent MJ, et al. Radiotherapy plus concomitant and adjuvent temozolomide for glioblastoma. *N Engl J Med*. 2005;352(10):987–996.

3. Provenzale JM, Mukundan S, Barboriak DP. Diffusion-weighted and perfusion MR imaging for brain tumor characterization and assessment of treatment response. *Radiology*. 2006;239(3):632–649.

4. Sugahara T, Korogi Y, Kochi M, et al. Usefulness of diffusion-weighted MRI with echo-planar technique in the evaluation of cellularity in gliomas. *J Magn Reson Imaging*. 1999;9:53–60.

5. Lyng H, Haraldseth O, Rofstad EK. Measurements of cell density and necrotic fraction in human melanoma xenografts by diffusion weighted magnetic resonance imaging. *Magn Reson Med*. 2000;43(6):828–836.

6. Ellingson BM, Malkin MG, Rand SD, et al. Validation of functional diffusion maps (fDMs) as a biomarker for human glioma cellularity. *J Magn Reson Imaging*. 2010;31(3):538–548.

7. Ellingson BM, LaViolette PS, Rand SD, et al. Spatially quantifying microscopic tumor invasion and proliferation using a voxel-wise solution to a glioma growth model and serial diffusion MRI. *Magn Reson Med*. 2011;65(4):1131–1143.

8. Chenevert TL, Stegman LD, Taylor JM, et al. Diffusion magnetic resonance imaging: an early surrogate marker for therapeutic efficacy in brain tumors. *J Natl Cancer Inst*. 2000;92(24):2029–2036.

9. Hamstra DA, Chenevert TL, Moffat BA, et al. Evaluation of the functional diffusion map as an early biomarker of time-to-progression and overall survival in high-grade glioma. *Proc Nat Acad Sci*. 2005;102(46):16759–16764.

10. Moffat BA, Chenevert TL, Lawrence TS, et al. Functional diffusion map: A noninvasive MRI biomarker for early stratification of clinical brain tumor response. *Proc Nat Acad Sci*. 2005;102(15): 5524–5529.

11. Moffat BA, Chenevert TL, Meyer CR, et al. The functional diffusion map: An imaging biomarker for the early prediction of cancer treatment outcome. *Neoplasia*. 2006;8(4):259–267.

12. Hamstra DA, Galbán CJ, Meyer CR, et al. Functional diffusion map as an early imaging biomarker for high-grade glioma: correlation with conventional radiologic response and overall survival. *J Clin Oncol*. 2008;26(10):3387–3394.

13. Reese TG, Heid O, Weisskoff RM, Wedeen VJ. Reduction of eddy-current-induced distortion in diffusion MRI using a twice-refocused spin echo. *Magn Reson Med*. 2003;49(1):177–182.

14. Cox RW, Jesmanowicz A. Real-time 3D image registration for functional MRI. *Magn Reson Med*. 1999;42:1014–1018.

15. Ellingson BM, Malkin MG, Rand SD, Bedekar DP, Schmainda KM. Functional diffusion maps applied to FLAIR abnormal areas are valuable for the clinical monitoring of recurrent brain tumors. *Proc Intl Soc Mag Reson Med*. 2009;17:285.

16. Ellingson BM, Malkin MG, Rand SD, et al. Comparison of cytotoxic and anti-angiogenic treatment responses using functional diffusion maps in FLAIR abnormal regions. *Proc Intl Soc Mag Reson Med*. 2009;17:1010.

17. Ellingson BM, Malkin MG, Rand SD, et al. Volumetric analysis of functional diffusion maps (fDMs) is a predictive imaging biomarker for cytotoxic and anti-angiogenic treatments in malignant gliomas. *J Neurooncol*. 2010. In Press.

18. Ellingson BM, Rand SD, Malkin MG, Schmainda KM. Utility of functional diffusion maps to monitor a patient diagnosed with gliomatosis cerebri. *J Neurooncol*. 2010;97(3):419–423.

19. Earnest F, 4th, Kelly PJ, Scheithauer BW, et al. Cerebral astrocytomas: histopathologic correlation of MR and CT contrast enhancement with stereotactic biopsy. *Radiology*. 1988;166(3): 823–827.

20. Kelly PJ, Daumas-Duport C, Kispert DB, Kall BA, Scheithauer BW, Illig JJ. Imaging-based stereotaxic serial biopsies in untreated intracranial glial neoplasms. *J Neurosurg*. 1987;66(6):865–874.

21. Kelly PJ, Daumas-Duport C, Scheithauer BW, Kall BA, Kispert DB. Stereotactic histological correlations of computed tomography- and magnetic resonance imaging-defined abnormalities in patients with glial neoplasms. *Mayo Clin Proc*. 1987;62(6):450–459.

22. Watanabe M, Tanaka R, Takeda N. Magnetic resonance imaging and histopathology of cerebral gliomas. *Neuroradiology*. 1992;34(6): 463–469.

23. Brant-Zawadski M, Norman D, Newton TH. Magnetic resonance imaging of the brain: the optimal screening technique. *Radiology*. 1984;152:71–77.

24. Byrne TN. Imaging of gliomas. *Semin Oncol*. 1994;21:162–171.

25. Husstedt HW, Sickert M, Köstler H, Haubitz B, Becker H. Diagnostic value of the fast-FLAIR sequence in MR imaging of intracranial tumors. *Eur Radiol*. 2000;10(5):745–752.

26. Tsuchiya K, Mizutani Y, Hachiya J. Preliminary evaluation of fluid-attenuated inversion-recovery MR in the diagnosis of intracranial tumors. *AJNR Am J Neuroradiol*. 1996;17(6):1081–1086.

27. Essig M, Hawighorst H, Schoenberg SO, et al. Fast fluid-attenuated inversion-recovery (FLAIR) MRI in the assessment of intraaxial brain tumors. *J Magn Reson Imaging*. 1998;8(4):789–798.

28. Dessouky BAM, El Abd OL, El Gowily AG, El Khawalka YM. Functional diffusion map of malignant brain tumors: A surrogate imaging biomarker for early prediction of therapeutic response and patient survival. *Egypt J Radiol Nucl Med*. 2010; 41:441–451.

29. Padhani AR, Liu G, Mu-Koh D, et al. Diffusion-weighted magnetic resonance imaging as a cancer biomarker: consensus and recommendations. *Neoplasia*. 2009;11(2):102–125.

30. Ellingson BM, Cloughesy TF, Lai A, Nghiemphu PL, Pope WB. Nonlinear registration of diffusion-weighted images improves clinical sensitivity of functional diffusion maps in recurrent glioblastoma treated with bevacizumab. [published online ahead of print June 23, 2011] *Magn Reson Med*. 2011.